

# NONLINEAR, REDUCED ORDER, DISTRIBUTED STATE ESTIMATION IN MICROGRIDS

Shivam Saxena<sup>†</sup>, Amir Asif<sup>‡</sup>, and Hany Farag<sup>†</sup>

<sup>†</sup>Electrical Engineering and Computer Science, York University, Toronto, ON, Canada M3J 1P3

<sup>‡</sup>Electrical and Computer Engineering, Concordia University, Montreal, QC, Canada H3J 1P8

## ABSTRACT

Recent developments in microgrids place strict constraints on the underlying state estimation technology, including the need for a dynamic and distributed approach. Since the problem is reminiscent of classical information fusion [2], the paper explores the application of a fusion-based reduced order, distributed unscented particle filter (FR/DUPF) for dynamic state estimation in microgrids. By partitioning the nonlinear microgrid into a network of  $n_{\text{sub}}$  localized and dynamically coupled systems, the FR/DUPF provides computational savings of a factor of  $n_{\text{sub}}$  over its centralized version. Monte Carlo simulations verify its accuracy by confirming that estimates from the FR/DUPF and centralized filter evolve close to the ground truth.

**Index Terms**— Microgrids, Islanded grids, Distributed estimation, Nonlinear estimation, Particle filters, Distributed generation.

## 1. INTRODUCTION

In power engineering, the existing electric power grid (EPG) framework is steadily being transformed into a new grid paradigm, referred to as the smart(er) power grid. Used to *deliver* power from a few generating plants to a large number of users, legacy EPGs operate as three level hierarchical systems (with the transmission, local sub-transmission, and distribution levels) and only allow for one-way power flow. Failure of a single EPG component, especially at the transmission or sub-transmission levels, has the potential of triggering massive power disruptions, as was the case in the U.S. Northeast blackout of 2003 that literally affected millions of consumers. Due to the need to generate large amounts of electricity at short notices at a few isolated stations, legacy EPGs depend on fossil fuel driven backup generators, which produce extreme amounts of carbon emissions. The emerging smart grid technology is being designed to address these issues. In response to smart grid initiatives, distribution networks should be able to host new components, technologies, and a wide variety of distributed and renewable generators (DG), energy storage devices, advanced grid control devices, advanced metering infrastructure, demand side management, and two way communication. Distribution networks are thus undergoing a major transition from being passive with unidirectional power flow toward active distribution networks (ADN) with multi-directional power and information flow. Meanwhile, widespread implementation of the DG is creating electrical regions with enough generation capacities to meet all or most of its local demand. Referred to as microgrids, these electrical regions have the ability to cut (island) themselves off from the parent grid, for example, in the case of a local failure. The microgrids allow for two-way electrical flows creating their own *delivery and storage* reservoirs. Hydrogen tanks and fuel cells replacing the backup diesel generators perform double-duty, i.e., release power on the grid from hydrogen at peak demand and in a reverse mode store

power by making hydrogen from electricity during off-peak hours.

Incorporating the aforementioned two-way power and information flow, and demand response features in smart power grids calls for timely knowledge of the operating status of the system based on real-time observations. Unlike state estimation in legacy EPGs [17]-[20], where state estimates are either static or updated only once every few minutes (mainly to reduce the computational complexity of the EPG estimator), smart grids in general and microgrids in particular require accurate and dynamic state updates, at times within a fraction of a second. For instance, when microgrids operate in the islanded mode, dispatchable DG units become responsible for holding the microgrid frequency and voltage amplitudes. Further, in typical microgrids, the interface between the DG units prime movers and the distribution systems is often based on power electronic converters acting as voltage sources. This kind of interface lacks the physical inertia that is typically available in the synchronous generators rotating masses. The lack of physical inertia in turn introduces a high level of susceptibility in the microgrid systems to parameter variations, system disturbances and load/generation variability. Therefore, one of the most important challenges related to ADNs is the realization of microgrids concept with the consideration of its special features and operational characteristics. Two recent studies [3, 4] have applied distributed state estimation to microgrids, however, the underlying power flow model used for estimation is static, limiting the accuracy of the estimator. Other studies [6-8],[13],[14] using a dynamical state model are based on the extended Kalman filter, whose limitations (lack of optimality, linearization error, and slow convergence) when applied to non-linear systems are quite well known. Reference [2] suggests more advanced Kalman filter based solutions, such as the second-order extended Kalman filter and unscented Kalman filter, but the exact implementations for state estimation in microgrids are not yet available. This paper takes a different approach and applies a distributed implementation of the unscented particle filter (UPF) [21]-[32] for state estimation in microgrids. Monte Carlo approaches such as the particle filter have been less explored in the context of state estimation in power grids due to the computational complexity involved despite their inherent ability to deal with nonlinear system dynamics and non-Gaussian noise models. Our UPF approach partitions the microgrid into  $n_{\text{sub}}$  coupled subsystems on the basis of the underlying microgrid structure and exploits the sparseness in each microgrid state model to its advantage. Rather than estimating the complete microgrid state vector at each microgrid, a subset of states relevant to the microgrid is instead estimated. The state variables estimated at each microgrid are largely different and those which are shared achieve consistency through a consensus step. The resulting fusion-based reduced order, distributed unscented particle filter (FR/DUPF) [12] limits the amount of information shared between neighbouring microgrids, reduces communication overhead, and provides computational savings of an order

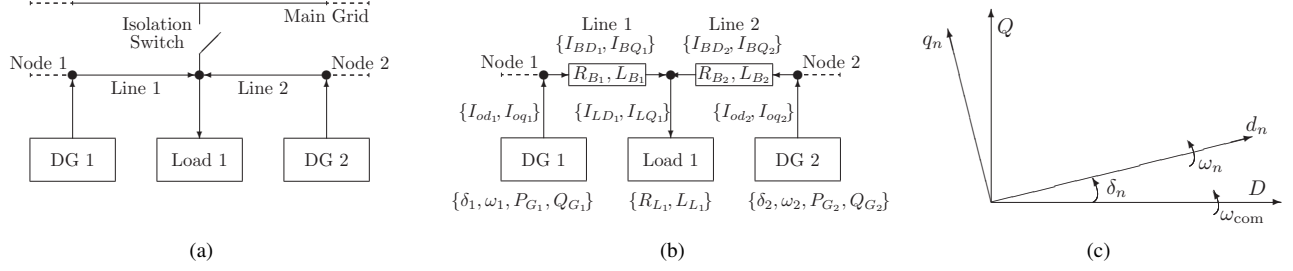


**Fig. 1:** (a) Illustrative example of a microgrid; (b) Equivalent network for the microgrid in (a); (c) DQ reference frame used in power networks.

of  $n_{\text{sub}}$  over the centralized particle filter. Our Monte Carlo simulations verify that the FR/DUPF is near-optimal and follows its centralized version closely. In [12], we derived the FR/DUPF algorithm for dynamic state estimation in legacy EPGs. Here, we extend the FR/DUPF to microgrids for reduced order state estimation.

In terms of the organization of this paper, Section 2 introduces the state-space dynamics for microgrids. In Section 3, we present a reduced-order model for the microgrid followed by the derivation of the proposed FR/DUPF in Section 4. Results from Monte Carlo simulations are presented in Section 5. Section 6 concludes the paper.

## 2. NON-LINEAR SYSTEM MODEL FOR MICROGRIDS

In distributed generation, a combination of renewable energy sources combine their power to satisfy large demands [9]. The voltages produced by these microsources are direct current (DC), which are converted to alternating current (AC) using a voltage inverter. Such a microgrid is classified as an inverter based microgrid and the generation units which produce power for the microgrid are called distributed generators (DG). The microgrid includes an isolation switch, which facilitates the connection of the microgrid to the main grid. With the isolation switch turned on, the microgrid is connected to the main grid with DGs injecting power to the bus. When the switch is off, the microgrid enters the islanded mode, where it is cut off from the main grid and services only its local power needs. A commonly known power sharing strategy called droop control is used to share power between different DGs to satisfy the overall load requirement.

Fig. 1(a) is an example of a section of a microgrid comprising two DGs and a load. Its equivalent network in the islanded mode is shown in Fig. 1(b). Each DG  $n$  supplies its output current  $\{I_{oD_n}, I_{oQ_n}\}$  to a node that connects the DG to the microgrid line. Modeled as a series resistor-inductor circuit, current  $\{I_{BD_l}, I_{BQ_l}\}$  flowing on line  $l$  is the accumulative difference of DG source currents  $\{I_{oD_n}, I_{oQ_n}\}$  and currents  $\{I_{LD_m}, I_{LQ_m}\}$  consumed by the loads connected to line  $l$ .

**DQ Reference Frame:** The voltages and currents in any AC power network have three phases in a stationary phase coordinate system (commonly referred to as the ABC frame). Since network analysis in the ABC frame is complex, it is transformed to another framework with two phases (direct and quad) rotating about an axis. The transformed frame is called the DQ frame and is symbolized as  $(d_n, q_n)$ . In a microgrid, each DG rotates at its own angular frequency  $\omega_n$  leading to several individual DQ frames. In order to analyze the overall system, all state variables in the microgrid are further transformed from their individual reference frames  $(d_n, q_n)$  to a reference DQ frame (typically the one associated with DG 1) by defining an angle  $\delta_n$ , which represents the phase difference between the individual  $(d_n, q_n)$  frame and the reference DQ frame. Since the reference DG is already aligned to the DQ axis, its angle is effectively zero. Using this fact, the rotational frequency can be calculated and is referred to as  $\omega_{\text{com}}$ , which in turn can be used to compute the phase angles

$\delta_n$  associated with every other DG in the network. Once the angle for each DG has been obtained, the state variables (say  $f_d, f_q$ ) of the individual DGs are mapped to  $(f_D, f_Q)$  in the reference DQ frame using the following transformation

$$\begin{bmatrix} f_D \\ f_Q \end{bmatrix} = \begin{bmatrix} \cos(\delta_n) & -\sin(\delta_n) \\ \sin(\delta_n) & \cos(\delta_n) \end{bmatrix} \begin{bmatrix} f_d \\ f_q \end{bmatrix} \quad (1)$$

**Modeling DGs:** In the simplified DG-inverter coupled model, each DG unit is modeled by a set of 5 state variables:  $\delta_n$  is the angle associated with DG  $n$ ;  $\{P_{G_n}, Q_{G_n}\}$  the active and reactive power generated by the DG;  $I_{oD_n}$  the output current in the  $d^{\text{th}}$  dimension, and;  $I_{oQ_n}$  the output current in the  $q^{\text{th}}$  dimension. The nonlinear state model for DG  $n$  consists of the following equations

$$\dot{\delta}_n(t) = \omega_n^* - M_{p_n} P_{G_n} - \omega_{\text{com}} \quad (2)$$

$$\dot{P}_{G_n}(t) = 1.5\omega_{c_n} [V_{o_n}^* - N_{q_n} Q_{G_n} I_{oD_n}] - \omega_{c_n} P_{G_n} \quad (3)$$

$$\dot{Q}_{G_n}(t) = 1.5\omega_{c_n} [V_{o_n}^* I_{oQ_n} - N_{q_n} Q_{G_n} I_{oQ_n}] - \omega_{c_n} Q_{G_n} \quad (4)$$

$$L_{c_n} \dot{I}_{oD_n}(t) = -R_{c_n} I_{oD_n} + \omega_{\text{com}} I_{oQ_n} L_{c_n} + V_{oD_n} - V_{bD_n} \quad (5)$$

$$L_{c_n} \dot{I}_{oQ_n}(t) = -R_{c_n} I_{oQ_n} - \omega_{\text{com}} I_{oD_n} L_{c_n} + V_{oQ_n} - V_{bQ_n} \quad (6)$$

where  $\omega_n^*$  is the DG output voltage angular frequency;  $\{M_{p_n}, N_{q_n}\}$  the active and reactive droop gain;  $\omega_{c_n}$  the cutoff frequency of the output filter;  $V_{o_n}^*$  the nominal output voltage magnitude set point;  $R_{c_n}$  the resistance of the output filter; and  $L_{c_n}$  the inductance of the output filter. These parameters are all constants. Symbol  $\dot{\cdot}$  at the top of variables (e.g., in  $\dot{\delta}_n(t)$ ) denotes derivation with respect to time  $t$ . Originally expressed in the local  $dq$  frame, the DG parameters in (2)-(6) are transformed to the reference DQ frame using (1).

Parameters  $\{V_{bD_p}, V_{bQ_p}\}$  are the DQ-components of the nodal voltage at node  $p$ . To ensure the solution of the microgrid network is well grounded, a virtual resistor  $R_p$  of a high value ( $1M\Omega$ ) is placed at each node [11]. Using the Kirchoff's current law, the nodal voltage is

$$V_{bD_p} = R_p \left( \sum I_{oD_{p(\text{in})}} + \sum I_{BD_{p(\text{in})}} - \sum I_{BD_{p(\text{out})}} - \sum I_{LD_{p(\text{out})}} \right) \quad (7)$$

$$V_{bQ_p} = R_p \left( \sum I_{oQ_{p(\text{in})}} + \sum I_{BQ_{p(\text{in})}} - \sum I_{BQ_{p(\text{out})}} - \sum I_{LQ_{p(\text{out})}} \right) \quad (8)$$

where subscript '(in)' denote current entering the node and '(out)' current leaving the node. For example, notation  $\{\sum I_{oD_{p(\text{in})}}, \sum I_{oQ_{p(\text{in})}}\}$  represent the DQ components of the accumulative current generated by DGs that enters node  $p$ . Likewise,  $\{\sum I_{LD_{p(\text{out})}}, \sum I_{LQ_{p(\text{out})}}\}$  represent the DQ components of the accumulative current consumed by loads that leaves node  $p$ . Other variables use similar notations.

**Modeling Distribution Lines:** The transmission lines connecting nodes are modeled as a series resistor-inductor circuit. For line  $l$ , the state variables are the line currents  $\{I_{BD_l}, I_{BQ_l}\}$  given by, [11],

$$L_{B_l} \dot{I}_{BD_l}(t) = -R_{B_l} I_{BD_l} + \omega_{\text{com}} L_{B_l} I_{BQ_l} + V_{BD_{l(\text{to})}} - V_{BD_{l(\text{from})}} \quad (9)$$

$$L_{B_l} \dot{I}_{BQ_l}(t) = -R_{B_l} I_{BQ_l} - \omega_{\text{com}} L_{B_l} I_{BD_l} + V_{BQ_{l(\text{to})}} - V_{BQ_{l(\text{from})}} \quad (10)$$

where  $R_{B_l}$  is the resistance of line  $l$  and  $L_{B_l}$  the inductance of line  $l$ . Also,  $V_{BD_{l(to)}}$  denotes the  $D$ -component of the voltage of the  $to$  bus and  $V_{BD_{l(from)}}$  the  $D$ -component of the voltage of the  $from$  bus.

**Modeling Loads:** The loads are modeled by their admittances. The states for load  $m$  are its current  $\{I_{LD_m}, I_{LQ_m}\}$  in the DQ frame

$$L_{L_m} \dot{I}_{LD_m}(t) = -R_{L_m} I_{LD_m} + \omega_{\text{com}} L_{L_m} I_{LQ_m} + V_{BD_m}(11)$$

$$L_{L_m} \dot{I}_{LQ_m}(t) = -R_{L_m} I_{LQ_m} - \omega_{\text{com}} L_{L_m} I_{LD_m} + V_{BQ_m}(12)$$

where  $\{R_{L_m}, L_{L_m}\}$  are the resistance and inductance of load  $m$ ,  $\{V_{BD_m}, V_{BQ_m}\}$  the DQ-components of the bus voltage connected to load  $m$  and  $\omega_{\text{com}}$  the rotational frequency of the reference DG.

### 2.1 Overall State and Observation Models

The overall state vector is formed by stacking all state variables corresponding to the DGs, lines, and loads in a vector

$$\mathbf{X}(t) = [\delta_n(t), P_{G_n}(t), Q_{G_n}(t), I_{oD_n}(t), I_{oQ_n}(t), I_{BD_1}, I_{BQ_1}(t), I_{LD_m}(t), I_{LQ_m}(t)]_{n,l,m}, \quad (13)$$

which leads to the a set of nonlinear ordinary differential equations

$$\dot{\mathbf{X}}(t) = \mathbf{f}(\mathbf{X}(t)) + \boldsymbol{\xi}(t) \quad (14)$$

based on (2)-(6) and (9)-(13), where vector  $\boldsymbol{\xi}(t)$  contains all input terms. The information used for estimation is a subset of active/reactive power flows, active/reactive power injections, and voltage/current magnitudes. We consider node voltages  $\{V_{bD_p}, V_{bQ_p}\}$ , (7)-(8), as measurements leading to the observation model

$$\mathbf{Z}(t) = \mathbf{g}(\mathbf{X}(t)) + \boldsymbol{\zeta}(t) \quad (15)$$

where  $\mathbf{Z}(t) = \{V_{bD_p}, V_{bQ_p}\}_p$  and  $\boldsymbol{\zeta}(t)$  the observation noise vector.

### 3. MICROGRIDS: REDUCED ORDER CONFIGURATION

In the proposed state estimator, the reduced-order state-space model is obtained by spatially decomposing the overall system into  $n_{\text{sub}}$  subsystems based on the observable states at each subsystem. In other words, the state model for Subsystem  $S^{(s)}$  consists of a subset of state variables  $\mathbf{X}^{(s)}(k) \subset \mathbf{X}(t)$  (referred to as the local state vector). A local observation vector  $\mathbf{Z}^{(s)}(t)$  is then attributed to Subsystem  $S^{(s)}$ , which is a collection of local measurements corresponding to the local state vector  $\mathbf{X}^{(s)}(t)$ . For such reduced-order subsystem  $S^{(s)}$ , ( $1 \leq s \leq n_{\text{sub}}$ ), the localized observation model is

$$\mathbf{Z}^{(s)}(t) = \mathbf{g}^{(s)}(\mathbf{X}^{(s)}(t)) + \boldsymbol{\zeta}^{(s)}(t). \quad (16)$$

The local state vectors in (16) may have shared states. The reduced-order state model (derived from (14) by partitioning) is then given by

$$\dot{\mathbf{X}}^{(s)}(t) = \mathbf{f}^{(s)}(\mathbf{X}^{(s)}(t), \mathbf{d}^{(s)}(t)) + \boldsymbol{\xi}^{(s)}(t). \quad (17)$$

where  $\mathbf{d}^{(s)}(t)$  is the coupling force term. When the overall system is partitioned into subsystems, the dynamical model for a subsystem may contain states that are directly observed by the subsystem and additional states that are not observed but are part of the global state model. The coupling force vector  $\mathbf{d}^{(s)}(t)$  includes states which are not directly observed but are part of the subsystem's model.

**Example:** In Fig. 2, we apply the partitioning approach to the microgrid test system of Fig. 1(a), which results in the following state, observation, and forcing terms' vectors for the two subsystems.

$$\begin{aligned} \text{State vectors: } \mathbf{X}^{(1)}(t) &= [\delta_1(t), P_{G_1}(t), Q_{G_1}(t), I_{oD_1}(t), \dots \\ & I_{oQ_1}(t), I_{BD_1}, I_{BQ_1}(t), I_{LD_1}(t), I_{LQ_1}(t)] \end{aligned}$$

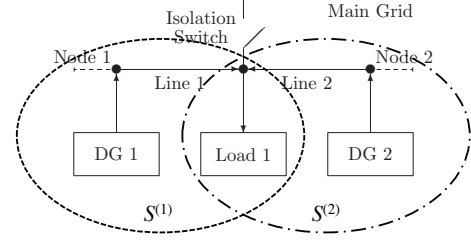


**Fig. 2:** Microgrid of Fig. 1 partitioned in 2 subsystems  $\{S^{(1)}, S^{(2)}\}$ .

$$\begin{aligned} \mathbf{X}^{(2)}(t) &= [\delta_2(t), P_{G_2}(t), Q_{G_2}(t), I_{oD_2}(t), \dots \\ & I_{oQ_2}(t), I_{BD_2}, I_{BQ_2}(t), I_{LD_1}(t), I_{LQ_1}(t)] \end{aligned}$$

$$\text{Observ. vectors: } \mathbf{Z}^{(1)}(t) = [V_{bD_1}(t), V_{bQ_1}(t), V_{bD_3}(t), V_{bQ_3}(t)]$$

$$\mathbf{Z}^{(2)}(t) = [V_{bD_2}(t), V_{bQ_2}(t), V_{bD_3}(t), V_{bQ_3}(t)]$$

$$\text{Forcing vectors: } \mathbf{d}^{(1)}(t) = [I_{BD_2}(t), I_{BQ_2}(t)],$$

$$\mathbf{d}^{(2)}(t) = [I_{BD_1}(t), I_{BQ_1}(t)].$$

The shared states between the subsystems are  $[I_{LD_1}(t), I_{LQ_1}(t)]$ . Each subsystem  $S^{(s)}$  runs its own local filter based on its subsystem state and observation model (16)-(17) to estimate its local state  $\mathbf{X}^{(s)}(t)$ . The forcing term  $\mathbf{d}^{(s)}(t)$  is received from the neighbouring node(s). A consensus algorithm maintains consistency in the shared states.

### 4. DISTRIBUTED PARTICLE FILTER IMPLEMENTATION

We apply the fusion-based reduced order, distributed unscented particle filter (FR/DUPF) [12] for state estimation in microgrids. Each subsystem  $S^{(s)}$  runs its local unscented particle filter (UPF) based on the discretized version of the localized models, (16)-(17). Index  $k$  is used instead of time  $t$  after the variables to denote their discretized values. Thus, local particles  $\mathbb{X}_i^{(s)}(k)$  and weights  $W_i^{(s)}(k)$ , ( $1 \leq i \leq N_s^{(s)}$ ), are associated with each subsystem  $S^{(s)}$ . Note that  $N_s^{(s)}$  denotes the number of particles associated with subsystem  $S^{(s)}$ . In addition, the particle update at each subsystem requires forcing terms  $\mathbf{d}^{(s)}(k)$  that are obtained from the neighbouring subsystems. The FR/DUPF consists of the following four steps.

**1. Local Particles Update via UPF:** The UPF couples the particle filter with the unscented Kalman filter (UKF). The optimal proposal distribution function is approximated as a Gaussian whose statistics (mean and covariance matrix) are computed using the UKF. All nodes estimate the state vector  $\hat{\mathbf{X}}^{(s)}(k)$  and covariance  $\hat{\mathbf{P}}^{(s)}(k)$  from their individual particle sets. See [12] for details.

**2. Weight Update using Observation Fusion:** The FR/DUPF approximates the weight update equation as a function of two terms: one depends on local state estimates and other on state estimates in the immediate neighbourhood as follows

$$\begin{aligned} W_i^{(s)}(k) &\propto W_i^{(s)}(k-1) P(\mathbf{z}(k) | \mathbb{X}_i^{(s)}(k), \hat{\mathbf{X}}^{(\neq s)}(k|k-1)) \\ &\times \frac{P(\mathbb{X}_i^{(s)}(k) | \mathbb{X}_i^{(s)}(k-1), \hat{\mathbf{X}}^{(\neq s)}(k-1))}{q(\mathbb{X}_i^{(s)}(k) | \mathbb{X}_i^{(s)}(k-1), \hat{\mathbf{X}}^{(\neq s)}(k-1), \mathbf{z}(k))}, \end{aligned} \quad (18)$$

where  $\hat{\mathbf{X}}^{(\neq s)}(\cdot)$  are estimates of the state variables *not* included in the local state vector  $\mathbf{X}^{(s)}(\cdot)$  for subsystem  $S^{(s)}$ . Eq. (18) still requires all observations from the entire network. Clearly, this is impractical. A further approximation is to limit the observation fusion to the neighboring nodes of  $S^{(s)}$ . This approximation works well due to the localized nature of the observations in the microgrids.

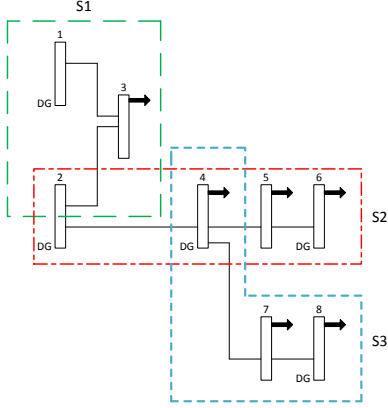


**Fig. 3:** Schematic for the 8-Bus, 5-DG, and 6-load microgrid used in our simulations. Each rectangle represents a bus labeled 1 to 8. Buses connected to a distributed generator has ‘DG’ written next to them. Buses connected to a load has a bold arrow pointing outwards.

**3. State Fusion:** For each shared state  $X_n(k)$ , Subsystem  $S^{(s)}$  estimates its mean  $\mu_n^{(s)}(k)$  and covariance  $P_n^{(s)}(k)$  from its weighted particles and applies the following fusion rule [14]

$$\hat{X}_n^{(\text{fuse})}(k) = \left( \sum [P_n^{(s)}(k)]^{-1} \right)^{-1} \left( \sum [P_n^{(s)}(k)]^{-1} \mu_n^{(s)}(k) \right), \quad (19)$$

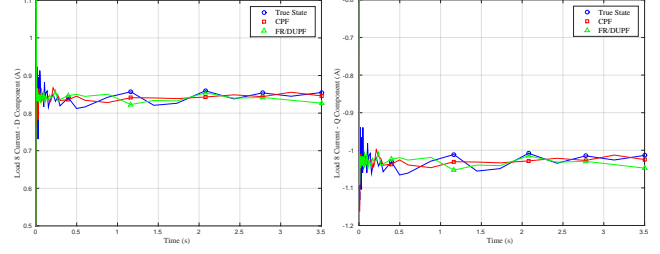
with covariance  $\hat{P}_n^{(\text{fuse})}(k) = \sum [P_n^{(s)}(k)]^{-1}$ . The summation terms in Eq. (19) are computed using average consensus [24] within immediate neighbourhoods of the nodes. Once the state fusion process for shared state  $X_n(k)$  is complete,  $S^{(s)}$  generates its local particles for  $X_n$  from the Gaussian distribution  $\mathcal{N}(\hat{X}_n^{(\text{fuse})}(k), \hat{P}_n^{(\text{fuse})}(k))$ .

**4. Computing Forcing Terms:** The final step in the FR/DUPF is to compute  $\mathbf{d}^{(s)}(k)$  and  $\hat{\mathbf{X}}^{(\neq s)}(k)$  for the next iteration. At this stage, all subsystems have consistent estimates for their shared states. Subsystem  $S^{(s)}$  requests the required forcing term  $\mathbf{d}^{(s)}(k)$  from its neighbours. This completes iteration  $k$  of the FR/DUPF.

**Computational Complexity:** The computational complexity [34] of the particle filter with  $n_x$  state variables and  $N_s$  vector particles of dimensions of  $(n_x \times 1)$  is of  $\mathcal{O}(n_x^2 N_s)$  flops. Partitioning the microgrid into  $n_{\text{sub}}$  subsystems, on average the number of state variables per subsystem is roughly  $n_x/n_{\text{sub}}$ . If  $N_s$  vector particles are maintained for each reduced state vector at the subsystems and assuming no shared state variables between subsystems, the complexity of the FR/DUPF is  $n_{\text{sub}} \times \mathcal{O}((n_x/n_{\text{sub}})^2 N_s) \approx \mathcal{O}(n_x^2 N_s/n_{\text{sub}})$  leading to a computational saving of a factor of  $n_{\text{sub}}$  in favour of the FR/DUPF.

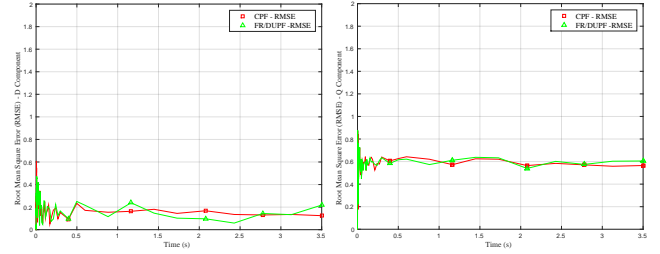
## 5. NUMERICAL SIMULATIONS

As a proof on concept, our simulation consists of implementing both the centralized and FR/DUPF particle filters on a 8-Bus, 5-DG microgrid test system shown in Fig. 3, which operates at 110V and at 60Hz frequency. The microgrid is configured for a black start, meaning that all state variables are set to zero at  $t = 0$ . The system model for the microgrid network is implemented in MATLAB and solved using MATLAB’s ode15 solver on an iteration by iteration basis. At each iteration, both state and observation vectors are corrupted with Gaussian noise at a signal to noise ratio (SNR) of 30dB. In the implementation of the centralized particle filter (CPF), all observations are assumed available at the fusion centre. There are 20 particles for each state variable to represent its posterior density, and with 51 state



(a) D-comp. of load current at Bus 8. (b) Q-comp. of load current at Bus 8.

**Fig. 4:** Comparison of the DQ-components of load current connected to Bus 8 estimated from the FR/DUPF and centralized particle filter with the ground truth for the microgrid shown in Fig. 3.



(a) RMS Error for Fig. 4(a).

(b) RMS Error for Fig. 4(b).

**Fig. 5:** Root mean square (RMS) errors for state estimates of Fig. 4.

variables, this leads to 1020 total particles being used for this filter. The observations are voltage magnitude readings in the DQ frame at each node based on the observation model (16).

Fig. 3 shows how the test microgrid is partitioned for the implementation of the FR/DUPF. The microgrid has been spatially decomposed into 3 subsystems  $\{S^{(1)}, S^{(2)}, S^{(3)}\}$ . The observation model is kept the same such that each bus in the subsystem is assumed to provide the voltage magnitude of that bus. A total of 12 shared states exist between the three subsystems. In order to maintain the same number of particles as in the centralized implementation, a total of  $1020/63 \approx 16$  particles/state were used in each subsystem in the FR/DUPF. As for the CPF, all states are initialized to zero.

Fig. 4 plots the estimated DQ-current waveforms for the load connected to Bus 8. Fig. 5 plots the corresponding RMS errors over a Monte Carlo simulation of 100 runs. It can be seen from the plots that both centralized and particle filters are correctly tracking the state values. The FR/DUPF is performing almost as well as the centralized particle filter. Given that the reduced order model is a near-optimal implementation and has a lower complexity, the FR/DUPF is proposed as an alternative to the centralized filter in microgrids.

## 6. CONCLUSION AND FUTURE WORK

We addressed the problem of nonlinear distributed data fusion in microgrids. The proposed FR/DUPF partitions the microgrid into several localized but coupled subsystems, and runs a reduced order particle filter on each subsystem. A consensus step ensures consistency among shared states across the microgrid. Compared to its centralized version, the FR/DUPF provides computational savings of up to the order  $n_{\text{sub}}$  of subsystems. Monte Carlo simulations verify the FR/DUPF as an acceptable alternative to the centralized filter. Future work will extend the single microgrid test system to a multi-microgrid system (IEEE 69 bus) under the smart grid paradigm; relax the full observability condition as measuring voltages at all nodes is impractical, and account for differences in scanning time and synchronization issues among instruments recording observations.

## 7. REFERENCES

- [1] A. Keyhani and M. Marwali. "Smart Power Grids 2011", Springer, 2011.
- [2] Y.F. Huang, S. Werner, J. Huang, N. Kashyap, and V. Gupta, "State Estimation in Electric Power Grids: Meeting new challenges presented by the requirements of the future grid," *IEEE Signal Processing Magazine*, vol. 29, no. 5, pp. 34-43, 2012.
- [3] Y. Hu, A. Kuh, A. Kavcic and D. Nakafuji, "Real-time State Estimation on Micro-grids," *The 2011 International Joint Conference on Neural Networks (IJCNN)*, pp. 1378-1385, 2011.
- [4] G. Korres, N.D. Hatziaargyriou and P. J. Katsikas, "State estimation in Multi-Microgrids," *European Transactions on Electrical Power*, vol. 21, no. 2, pp. 1178-1199, 2011.
- [5] I. Dzafic, S. Henselmeyer and H.T. Neisius, "High Performance State Estimation for Smart Grid Distribution Network Operation," *Innovative Smart Grid Technologies (ISGT)*, pp. 1-6, 2011.
- [6] Y. Wang, Y. Tian, X. Wang, Z. Chen and Y. Tan, "Kalman-Filter-Based state estimation for system information exchange in a multi-bus islanded microgrid," *7th IET International Conference on Power Electronics, Machines and Drives (PEMD 2014)*, pp. 1-6, 2014.
- [7] H. Ma, Y. Yang, Y. Chen and K.J. Liu, "Distributed State Estimation in Smart Grid with Communication Constraints," *Signal & Information Processing Association Annual Summit and Conference (APSIPA ASC)*, pp. 1-4, 2012.
- [8] Y. Weng, R. Negi, and M.D. Ilic, "Historical Data-Driven State Estimation for Electric Power Systems," *2013 IEEE International Conference on Smart Grid Communications (Smart-GridComm)*, pp. 97-102, 2013.
- [9] R. Lasseter, "Microgrids," *Proc. Power Eng. Soc. Winter Meeting*, vol. 1, pp. 305-308
- [10] H. Farag, M. Mohamed, and A. Abdelaziz, "Voltage and Reactive Power Impacts on Successful Operation of Islanded Microgrids," *IEEE Transactions on Power Systems*, vol. 28, no. 2, pp. 1716-1727, 2013
- [11] N. Pogaku, M. Prodanovic, and T. Green, "Modeling, Analysis and Testing of Autonomous Operation of an Inverter-Based Microgrid," *IEEE Transactions on Power Electronics*, vol. 22, no. 2, pp. 613-625
- [12] A. Asif, A. Mohammadi, and S. Saxena, Nonlinear State Estimation Algorithms for Electrical Power Grid, *IEEE Int. Conf. on Acoustics, Speech, and Signal Processing (ICASSP)*, 2014.
- [13] M.D. Ilic, Le Xie, U.A. Khan, J.M.F. Moura, "Modeling of Future Cyber Physical Energy Systems for Distributed Sensing and Control," *IEEE Transactions on Systems, Man and Cybernetics, Part A: Systems and Humans*, vol. 40, no. 4, pp. 825-838, 2010.
- [14] U.A. Khan and J.M.F. Moura, "Distributing the Kalman filter for large-scale systems," *IEEE Trans. on Signal Processing*, vol. 56, no.10, pp. 4919-4935, 2008.
- [15] Le Xie, Dae-Hyun Choi, S. Kar, H.V. Poor, "Fully Distributed State Estimation for Wide-Area Monitoring Systems," *IEEE Transactions on Smart Grid*, vol. 3, no. 3, pp. 1154-1169, 2012.
- [16] G.N. Korres, "A Distributed Multiarea State Estimation," *IEEE Transactions on Power Systems*, vol. 26, no. 1, pp. 73-84, 2011.
- [17] V. Kekatos and G.B. Giannakis, "Distributed Robust Power System State Estimation," *IEEE Transactions on Power Systems*, vol. 28, no. 2, pp. 1617-1626, 2013.
- [18] G.G. Rigatos and P. Siano, "Distributed state estimation for condition monitoring of nonlinear electric power systems," *IEEE Inter. Symp. Industrial Electronics*, pp.1703-1708, 2011.
- [19] M. Dehghani, S. Nikraves, "State-Space Model Parameter Identification in Large-Scale Power Systems," *IEEE Transactions on Power Systems*, vol. 23, no. 3, pp. 1449-1457, 2008.
- [20] M. Dehghani and S. K. Y. Nikraves, "Nonlinear state space model identification of synchronous generators," *Elect. Power Syst. Res.*, vol. 78, no. 5, pp. 926940, 2008.
- [21] N. Gordon, M. Sanjeev, S. Maskell, and T. Clapp, "A tutorial on particle filters for online nonlinear/non-gaussian bayesian tracking," *IEEE Trans. Sig. Proc.*, vol. 50, pp. 174-187, 2002.
- [22] M. Briers, A. Doucet and S. S. Singh, "Sequential auxiliary particle belief propagation", *Int. Conf. on Inf. Fusion*, pp. 705-711, 2005.
- [23] M.F. Bugallo, Ting Lu and P.M. Djuric, "Target Tracking by Multiple Particle Filtering," *Aerospace Conf.*, pp.1-7, 2007.
- [24] A. Mohammadi and A.Asif, "Distributed Particle Filter Implementation with Intermittent/Irregular Consensus Convergence," *IEEE Trans. on Sig. Proc.*, vol. 61, no. 10, pp. 2572-2587, May15, 2013.
- [25] \_\_\_\_\_, "Full Order Nonlinear Distributed Estimation in Intermittently Connected Networks", *IEEE Int. Conf. on Acoustics, Speech and Signal Proc. (ICASSP)*, 2013.
- [26] \_\_\_\_\_, "A Constraint Sufficient Stas based Distributed Particle Filter for Bearing Only Tracking", *IEEE International Conference on Communication (ICC)*, pp. 3670-3675, 2012.
- [27] \_\_\_\_\_, "Posterior Cramer-Rao Bounds for Full and Reduced-order Distributed Bayesian Estimation," accepted in *IEEE Transactions on Aerospace and Electronic Systems*, 2013. manuscript of 38 pages. in press.
- [28] O. Hlinka, F. Hlawatsch, and P.M. Djuric, "Distributed Particle Filtering in Agent Networks: A Survey, Classification, and Comparison," *IEEE Signal Processing Magazine*, vol. 30, no. 1, pp. 61-81, Jan. 2013.
- [29] S. Farahmand, S. I. Roumeliotis, and G. B. Giannakis, "Set-membership constrained particle filter: Distributed adaptation for sensor networks, *IEEE Trans. on Signal Processing*, vol. 59, no. 9, pp. 4122-4138, Sept. 2011.
- [30] D. Ustebay, M. Coates, and M. Rabbat, "Distributed auxiliary particle filters using selective gossip," *IEEE Int. Conf. Acoustics, Speech and Signal Proc. (ICASSP)*, pp. 3296-3299, 2011.
- [31] A. Mohammadi and A. Asif, "Distributed State Estimation for Large-scale Nonlinear Systems: A Reduced Order Particle Filter Implementation," *IEEE Statistical Sig. Proc. (SSP)*, pp. 249-252, 2012.
- [32] A. Mohammadi and A. Asif, "Distributed particle filtering for large scale dynamical systems," In *IEEE 13th Inter. Multitopic Conference*, pp.1-5, 2009.
- [33] T.M. Berg and H.F. Durrant-Whyte, "Model distribution in decentralized multi-sensor data fusion," *American Cont. Con.*, pp. 2292-2293, 1991.
- [34] R. Karlsson, T. Schon, and F. Gustafsson, "Complexity Analysis of the Marginalized Particle Filter," *IEEE Trans. Signal Processing*, vol. 53, no. 11, pp. 4408-4411, 2005.